Composition of Safety Constraints With Applications to Decentralized Fixed-Wing Collision Avoidance

Eric Squires, Pietro Pierpaoli, Rohit Konda, Samuel Coogan, and Magnus Egerstedt

***Abstract*—In this paper we discuss how to construct a barrier certificate for a control affine system subject to actuator constraints and motivate this discussion by examining collision avoidance for fixed-wing unmanned aerial vehicles (UAVs). In particular, the theoretical development in this paper is used to create a barrier certificate that ensures that two UAVs will not collide for all future times assuming the vehicles start in a safe starting configuration. We then extend this development by discussing how to ensure that multiple safety constraints are simultaneously satisfied in a decentralized manner (e.g., ensure robot distances are above some threshold for all pairwise combinations of UAVs for all future times) while ensuring output actuator commands are within specified limits. We validate the theoretical developments of this paper in the simulator SCRIMMAGE with a simulation of 20 UAVs that maintain safe distances from each other even though their nominal paths would otherwise cause a collision.**

***Index Terms*—Barrier function, safety, multi-agent systems, fixed-wing unmanned aerial vehicles.**

I. Introduction

As low-cost, unmanned aerial vehicles (UAVs) find civilian uses, the low-altitude airspace is increasingly congested, leading to large-scale UAV operation limitations including concerns for privacy, the environment, national security, and safe-flight validation [1]. A key challenge for safe-flight validation in congested environments is ensuring collision avoidance while enabling vehicles to accomplish their designed missions. Thus, in this paper we propose a decentralized algorithm that minimally alters a vehicle's nominal control signal (designed, for example, to deliver goods or for crop monitoring) while still ensuring safe operations.

Eric Squires (corresponding author) is with the Georgia Tech Research Institute, 250 14th Street, NW Atlanta, GA 30332, USA (e-mail: eric.squires@gtri.gatech.edu).

Pietro Pierpaoli is with the School of Electrical and Computer Engineering, Georgia Institute of Technology, Atlanta, GA 30332, USA (e-mail: pietro.pierpaoli@gatech.edu)

Rohit Konda is with the School of Electrical and Computer Engineering, Georgia Institute of Technology, Atlanta, GA 30332, USA (e-mail: rkonda6@gatech.edu)

Sam Coogan is with the School of Electrical and Computer Engineering as well as the School of Civil and Environmental Engineering, Georgia Institute of Technology, Atlanta, GA 30332, USA (email: sam.coogan@gatech.edu)

Magnus Egerstedt is with the School of Electrical and Computer Engineering, Georgia Institute of Technology, Atlanta, GA 30332, USA (e-mail: magnus.egerstedt@ece.gatech.edu)

The work by Magnus Egerstedt and Pietro Pierpaoli was supported by Grant No. ARL DCIST CRA W911NF-17-2-0181 by the US Army Research Lab. The work of Sam Coogan and Rohit Konda was supported by the Air Force Office of Scientific Research under grant number FA9550-19-1-0015.

A variety of approaches to fixed-wing collision avoidance have been proposed. Partially observable Markov decision processes are used in [2], [3] to achieve safe flight distances. The dynamic window approach, originally introduced in [4] for static obstacles and adapted to moving obstacles in [5], uses circular arcs for trajectories and limits the set of allowable velocities to enable a quick optimization of the control input. In [6], the authors develop a first-order look-ahead algorithm that can be applied to vehicles with unicycle dynamics in a decentralized way while guaranteeing that collisions amongst k vehicles are avoided. Potential functions [7], [8] have also been applied to fixed-wing collision avoidance, where it can be shown that vehicles can safely avoid each other even when their sensing range is limited. Similarly, [9] discusses how to combine potential functions with trajectory goals into a navigation function in order to provide criteria under which collision avoidance can be guaranteed. Navigation functions have also been combined with Model Predictive Control (MPC) by making inter-agent distance requirements implicit in the cost function [10]. MPC has additionally been applied to UAV collision avoidance for vehicles with limited sensing [11] and communication constraints [12]. While MPC provides a flexible framework for distributed collision avoidance, its limited horizon can make safety guarantees difficult. In a more general case, the optimal control formulation in [13] allows for collision avoidance guarantees, but it is computationally intensive as it requires numerically solving the Hamilton-Jacobi-Bellman equations over an infinite horizon.

A central idea of this paper is how to leverage evasive maneuvers to guarantee safe operations. Trajectory generation was analyzed in [14] where a nonlinear program is developed to find a safe reference trajectory constructed from polynomials. In [15] and [16], the authors discuss trajectory generation using a RRT with dynamics constraints provided by dubins paths and a waypoint generation algorithm, respectively.

Similar to evasive maneuvers, traffic rules [17], [18] are a method for encoding hybrid behaviors that can include collision avoidance trajectories. In [17], the authors show that a two vehicle system with limited sensing range can avoid collisions while reaching position goals. While in general this may result in conservative behaviors, they demonstrate in simulation that the decentralized algorithm continues to allow vehicles to reach their target configuration while avoiding collisions for as many as 70 vehicles.

Motivated by the importance of formal guarantees of collision avoidance that are computationally feasible and minimally invasive we discuss in this paper how to apply barrier certificates (e.g., [19], [20]) to the UAV collision avoidance problem, where the system is subject to actuator constraints, nonlinear dynamics, and nonlinear safety constraints. Barrier certificates provide guarantees that a system will stay safe (i.e., vehicles will maintain safe distances from each other) for all future times. Further, under some assumptions detailed in Section II, barrier certificates can be formulated as a Quadratic Program (QP) for fast online computation of safe control inputs [20]. Given such safety guarantees, barrier certificates have been applied to a set of problems including collision avoidance for autonomous agents ([21], [22]), bipedal robots ([23], [24]), adaptive cruise control and lane following ([25], [20], [26], [27]), and in mobile communication networks [28].

However, barrier certificates rely on being able to find a function for safety set invariance to be guaranteed. For systems like a fixed wing UAV with actuator constraints, nonlinear dynamics, and nonlinear safety constraints, generating such a function can be difficult. In this respect they are similar to Lyapunov functions. They provide guarantees when a system designer can find appropriate functions but they may be difficult to construct.

Nevertheless, there are a variety of approaches to finding a barrier certificate given a system and safety constraints. One approach discussed for instance in ([25], [29], [19], [30]), uses a sum of squares decomposition [31]. In this approach an initially conservative estimate for a barrier certificate is found and the associated safe set is iteratively enlarged. Iterative approaches have also been developed when the system has relative degree greater than one. The conditions for calculating a safe control input for higher order systems are given in [32]. In [24], a backstepping approach is developed that ensures a control barrier certificate can be constructed and a similar approach is discussed in [33]. In both cases, the barrier function construction requires that the control input is not subject to actuator constraints.

System-specific arguments have also been applied to the development of a barrier certificate. For instance, geometric insights are exploited in [23], where the authors develop a barrier function for precise foot placement by ensuring that foot is within the intersection of two circles. Similarly, in [21], [22], the authors develop a barrier function that ensures a circle and ellipsoid, respectively, around each robot will not overlap in order to ensure there will be no collisions for double integrator and quadrotor robots, respectively. Barrier certificates have also been developed for unicycle dynamics in [27], where the dynamics are simplified by considering a point slightly in front of the vehicle.

This paper is concerned with ensuring that fixed-wing UAVs maintain safe distances from each other. Because collision avoidance can be viewed as a constraint for each pairwise combination of vehicles [28], [34], we briefly review how barrier certificates have been applied to systems with multiple constraints. A contract-based approach is presented in [25]. A sum of squares decomposition is presented in [30] where additional safety constraints map to additional constraints in the optimization problem. In [33], necessary and sufficient conditions are given for the existence of a control input that satisfies multiple barrier certificate constraints. The approach generalizes to high order and time-varying systems but requires that actuator constraints be unbounded. Barrier certificate composition has also been addressed in [25], [28], and [34]. In [25], the authors partition the state space into regions for which a single barrier certificate is active in each component of the partition. In [28] and [34] non-smooth barrier functions are discussed, where the result allows for combining barrier certificates using boolean primitives. One drawback of the boolean composition approaches is that it is not guaranteed that the composition of barrier functions will result in a barrier function.

This paper makes the following contributions. First, it generalizes a method discussed for instance in [21], [22] for constructing a barrier certificate that can be used to make safety guarantees for a system. Second, it shows how to ensure that multiple safety constraints can be satisfied simultaneously when using this constructive method. Third, it presents a decentralized algorithm for ensuring safety in the context of multi-agent systems. Fourth, it shows how to apply the above theory to a scenario involving fixed wing UAVs where vehicles must ensure minimum separation distances are maintained at all times. This paper expands on the conference version [35] which did not consider multiple constraints and only considered the centralized case. It also expands on the simulation study presented in [35] by considering a scenario with 20 vehicles to demonstrate that all pairwise distances between vehicles can be kept above a minimum safety distances throughout a scenario.

This paper is organized as follows. Section II discusses background information for barrier certificates. Section III discusses a general method for constructing a barrier certificate and shows how to apply it to fixed wing collision avoidance. Section IV generalizes the results of Section III by showing how to satisfy multiple constraints simultaneously. Section V relaxes the amount of information required to share between vehicles while still guaranteeing safety. Section VI presents a simulation verification of the approach. Section VII concludes.

II. BARRIER CERTIFICATES BACKGROUND

We summarize the necessary background for barrier certificates here. See [20] for a more complete discussion. Consider a control affine system

$$\dot{x} = f(x) + g(x)u \tag{1}$$

where f and g are locally Lipschitz, $x \in \mathbb{R}^n$, $u \in U \subseteq \mathbb{R}^m$, and solutions are forward complete, meaning the system has a unique solution for all time greater than or equal to 0 given a starting condition $x(0)$.

To use this formation for a set of vehicles, suppose there are k vehicles with state x_i and dynamics $\dot{x}_i = f_i(x_i) + g_i(x_i)u_i$ where $x_i \in \mathbb{R}^{n_i}, u_i \in U_i \subseteq \mathbb{R}^{m_i}$ and $i \in \{1, \ldots, k\}$. The overall state is $x = \begin{bmatrix} x_1^T & x_2^T & \cdots & x_k^T \end{bmatrix}^T \in \mathbb{R}^n$ where $n = \sum_{i=1}^k n_i$ and $u = \begin{bmatrix} u_1^T & u_2^T & \cdots & u_k^T \end{bmatrix}^T \in U_1 \times U_2 \times \cdots \times$

$U_k = U \subseteq \mathbb{R}^m$ where $m = m_1 + \cdots + m_k$. In this case, (1) can be represented as

$$\dot{x} = \begin{bmatrix} f_1(x_1) \\ f_2(x_2) \\ \vdots \\ f_k(x_k) \end{bmatrix} + \begin{bmatrix} g_1(x_1) & 0 & \cdots & 0 \\ 0 & g_2(x_2) & \cdots & 0 \\ \vdots & \vdots & \ddots & \vdots \\ 0 & 0 & \cdots & g_k(x_k) \end{bmatrix} \begin{bmatrix} u_1 \\ u_2 \\ \vdots \\ u_k \end{bmatrix}.$$

In this paper we model the individual vehicles with state $x_i = \begin{bmatrix} p_{i,x} & p_{i,y} & \theta_i \end{bmatrix}^T$ and $u_i = \begin{bmatrix} v_i & \omega_i \end{bmatrix}^T$ with dynamics

$$\dot{x}_i = \begin{bmatrix} \cos(\theta_i) & 0 \\ \sin(\theta_i) & 0 \\ 0 & 1 \end{bmatrix} \begin{bmatrix} v_i \\ \omega_i \end{bmatrix}, \tag{2}$$

where $v_i \in [v_{min}, v_{max}]$ with $v_{min} > 0$ and $|\omega_i| \leq \omega_{max}$. Let $h : \mathbb{R}^n \to \mathbb{R}$ be an output function, $\mathcal{D} \subset \mathbb{R}^n$ an open set, and denote the superlevel set

$$\mathcal{C}_h = \{x \in \mathcal{D} \,:\, h(x) \geq 0\}. \tag{3}$$

Definition 1. [20] Given a set $\mathcal{C}_h \subset \mathbb{R}^n$ defined in (3) for a continuously differentiable function $h : \mathbb{R}^n \to \mathbb{R}$, the function h is called a *zeroing control barrier function (ZCBF)* defined on a set $\mathcal{D}$ with $\mathcal{C}_h \subseteq \mathcal{D} \subset \mathbb{R}^n$, if there exists a Lipschitz continuous extended class $\mathcal{K}$ function α such that

$$\sup_{u \in U} [L_f h(x) + L_g h(x) u + \alpha(h(x))] \geq 0, \; \forall x \in \mathcal{D}. \tag{4}$$

In the above definition $L_f h$ and $L_g h$ denote the Lie derivatives. The admissible control space is defined as

$$K_h = \{u \in U \;:\; L_f h(x) + L_g h(x) u + \alpha(h(x)) \geq 0\}. \tag{5}$$

Theorem 1. *[20] Given a set $\mathcal{C}_h \subseteq \mathbb{R}^n$ defined in (3) for a continuously differentiable function h, if h is a ZCBF on $\mathcal{D}$, then any Lipschitz continuous controller $u : \mathcal{D} \to U$ such that $u(x) \in K_h(x)$ will render the set $\mathcal{C}_h$ forward invariant.*

In [20] it is also shown how to calculate $u(x) \in K_h(x)$ using a Quadratic Program (QP) to support fast, online calculations. In particular, assume there is some nominal $\hat{u}$ available that is designed to achieve some performance goal (e.g., path-following) that has not necessarily been designed to satisfy safety constraints. Additionally, we assume U can be expressed as the set of all u satisfying the linear inequality $Au \geq b$. The safe control input can then be calculated using a QP as follows

$$u^* = \min_{u \in \mathbb{R}^m} \frac{1}{2} \|u - \hat{u}\|^2 \tag{6a}$$

$$\text{s.t.} \quad L_f h(x) + L_g h(x) u + \alpha(h(x)) \geq 0 \tag{6b}$$

$$Au \geq b. \tag{6c}$$

Note that by property (4), when h is a ZCBF, (6) is guaranteed to be feasible when $x \in \mathcal{D}$.

III. Barrier Certificate Construction

A. Motivating Example

In this section we discuss some difficulties with applying barrier certificates to the fixed-wing collision avoidance problem via a concrete example. Consider a candidate ZCBF, h, that encodes a collision avoidance safety constraint

$$h(x(t)) = d_{1,2}(x) - D_s^2, \tag{7}$$

where $d_{1,2}(x) = (p_{1,x}(t) - p_{2,x}(t))^2 + (p_{1,y}(t) - p_{2,y}(t))^2$ is the squared distance between vehicles 1 and 2 and D_s is a minimum safety distance.

One common approach for systems with relative degree equal to one is to use the safety constraint directly as a ZCBF. However, when actuator constraints are present, the safety constraint may fail to be a valid ZCBF. To show why h defined in (7) is not a ZCBF, we present an example where $x \in \mathcal{C}_h$ but h does not satisfy (4). Let $x_1 = \begin{bmatrix} -D_s/2 & 0 & 0 \end{bmatrix}^T$ and $x_2 = \begin{bmatrix} D_s/2 & 0 & \pi \end{bmatrix}^T$ so that $x = \begin{bmatrix} x_1^T & x_2^T \end{bmatrix}^T \in C_h$ because $h(x) = 0$. Further,

$$\begin{aligned} &\sup_{u \in U} [L_f h(x) + L_g h(x) u + \alpha(h(x))] \\ &\quad = \sup_{u \in U} \big[2(p_{1,x}(t) - p_{2,x}(t))(v_1 \cos\theta_1(t) - v_2 \cos\theta_2(t)) \\ &\qquad + 2(p_{1,y}(t) - p_{2,y}(t))(v_1 \sin\theta_1(t) - v_2 \sin\theta_2(t)) \big] \\ &\quad = \sup_{u \in U} [-2D_s(v_1 + v_2)] \\ &\quad = -4 D_s v_{min}. \end{aligned}$$

Since $v_{min} > 0$ and $D_s > 0$, $\sup_{u \in U}[L_f h(x) + L_g h(x) u + \alpha(h(x))] < 0$ so h is not a ZCBF. The problem with this candidate ZCBF is that it does not account for the fact that by the time the vehicles are close to colliding, it may be too late to avoid each other due to the limited turning radius and positive minimum velocity.

B. Constructing a Barrier Certificate via Evading Maneuvers

In order to overcome the difficulties demonstrated in the example of Section III-A, we introduce a method to construct a ZCBF from a safety constraint. Let $\rho : \mathcal{D} \to \mathbb{R}$ be a *safety function* that represents the safety objective we want to satisfy at all times so that $\rho(x) \geq 0$ indicates that the system is safe. In the example from Section III-A for vehicles i and j,

$$\rho(x(t)) = d_{i,j}(x) - D_s^2. \tag{8}$$

Second, let $\gamma : \mathcal{D} \to U$ be a *nominal evading maneuver*. Section III-C discusses specific examples of γ for the UAV collision avoidance problem. For now, assuming γ has been selected, let

$$h(x(t); \rho, \gamma) = \inf_{\tau \in [0, \infty)} \rho(\hat{x}(t + \tau)), \tag{9}$$

be a candidate ZCBF where $\hat{x}$ and $\dot{\hat{x}}$ are given by

$$\hat{x}(t + \tau) = x(t) + \int_0^\tau \dot{\hat{x}}(t + \eta) d\eta, \tag{10}$$

$$\dot{\hat{x}}(t + \tau) = f(\hat{x}(t + \tau)) + g(\hat{x}(t + \tau))\gamma(\hat{x}(t + \tau)). \tag{11}$$

This choice of a candidate ZCBF h is motivated by the fact that in (9), h measures how close the state will get to the boundary of the safe set assuming γ is used as the control input for all future time. We first establish sufficient conditions under which h is differentiable. To do this, we assume that h has a unique x minimizer. In other words, there is a unique $x_{\min} \in \mathcal{D}$ such that $h(x) = \rho(x_{\min})$ where $x_{\min} = \hat{x}(t+\tau)$ for at least one $\tau \geq 0$. See the appendix for the proof.

Theorem 2. *Assume h is defined in (9) and is constructed from $\rho : \mathcal{D} \to \mathbb{R}$ and $\gamma : \mathcal{D} \to U$. Let h have a unique x minimizer for all $x \in \mathcal{D}$, ρ be continuously differentiable, and γ be such that $f(x) + g(x)\gamma(x)$ is continuously differentiable. Then h is continuously differentiable.*

Remark 1. For cases where the candidate ZCBF h has multiple x minima at $x_{\min_1}, \ldots, x_{\min_l}$ for some integer $l > 1$, the derivative will not necessarily be smooth. See [34] for handling this case.

In Section III-A we saw that we could not use the Euclidean distance for a ZCBF because when a candidate ZCBF h is defined as in (7), K_h could be empty even though h was non-negative. In other words, h could be non-negative but there was no control input available to keep the system safe. With h defined in (9), this problem is alleviated.

Theorem 3. *Assume h in (9) is continuously differentiable and γ is locally Lipschitz. Then h is a ZCBF on $\mathcal{C}_h$. If in addition, $L_g h(x)$ is non-zero for some $x \in \partial C_h$ and γ maps to values in the interior of U, then h is a ZCBF on a set $\mathcal{D}$ where $\mathcal{C}_h \subset \mathcal{D}$.*

Proof. We start by assuming $x \in \mathcal{C}_h$ and show that h satisfies (4). Because $x \in \mathcal{C}_h$, $h(x) \geq 0$ so $\alpha(h(x)) \geq 0$. Further, note that $L_f h(x) + L_g h(x)\gamma(x)$ is the derivative along the trajectory of $\hat{x}$. In other words,

$$
\begin{aligned}
&L_f h(x(t)) + L_g h(x(t))\gamma(x(t)) = \\
&\lim_{a \to 0^+} \frac{1}{a} \left(\inf_{\tau \in [a,\infty)} \rho(\hat{x}(t+\tau)) - \inf_{\tau \in [0,\infty)} \rho(\hat{x}(t+\tau)) \right).
\end{aligned} \tag{12}
$$

Consider the term inside the parenthesis in (12), namely

$$
\inf_{\tau \in [a,\infty)} \rho(\hat{x}(t+\tau)) - \inf_{\tau \in [0,\infty)} \rho(\hat{x}(t+\tau))
$$

and notice that it is the subtraction of an infimum of the same function ρ evaluated on two different intervals. Further, note that the first interval is a subset of the second interval since a approaches 0 from above. Thus, the term inside the parenthesis on the right hand side of (12) is non-negative so $L_f h(x) + L_g h(x)\gamma(x) \geq 0$. We can then conclude that $L_f h(x) + L_g h(x)\gamma(x) + \alpha(h(x)) \geq 0$ so $\gamma(x) \in K_h(x)$.

Now assume that $L_g h(x)$ is non-zero for some $x \in \partial C_h$ and γ maps to values in the interior of U. We will show that there is a set $\mathcal{D}$ that is a strict superset of $\mathcal{C}_h$ for which (4) holds. Let $x \in \partial \mathcal{C}_h$ be such that $L_g h(x)$ is non-zero and $B(x, \delta)$ be a ball of radius $\delta > 0$ such that for all $z \in B(x,\delta) \setminus \mathcal{C}_h$, $L_f h(z)$ is non-zero. Such a ball exists such that $B(x,\delta) \setminus \mathcal{C}_h$ is nonempty because $L_g h(x)$ is continuous. Let $d(z)$ be a non-zero vector such that $d(z) + \gamma(x) \in U$ where $d(z)$ is a non-zero vector in the direction of $L_g h(z)$. Note that such a vector exists because γ maps to the interior of U. Also note that $L_g h(z) d(z) > 0$. Further restrict δ so that $L_g h(z) d(z) + \alpha(h(z)) \geq 0$ for all $z \in B(x;\delta) \setminus \mathcal{C}_h$. Note that for similar reasons discussed earlier in the proof, $L_f h(z) + L_g h(z)\gamma(z) \geq 0$. Then

$$
\begin{aligned}
&L_f h(z) + L_g h(z)(\gamma(z) + d) + \alpha(h(z)) \\
&\quad \geq L_g h(x) d + \alpha(h(z)) \\
&\quad \geq 0.
\end{aligned}
$$

□

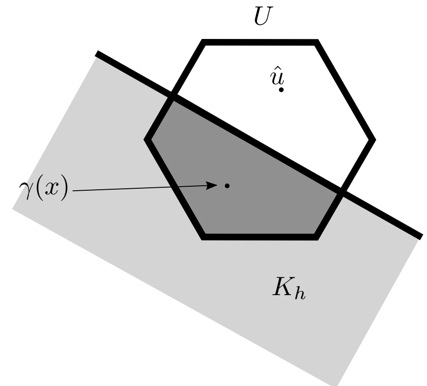

Fig. 1: A geometric view of why h defined in (9) can be a barrier function. Here U is shown as a closed convex polytope satisfying $U = \{u \ : \ Au \geq b\}$ and K_h is the half-space. The constraint (4) implies that the intersection of U and K_h is non-empty. When h is defined in (9), it satisfies this constraint by ensuring that $\gamma(x) \in U$ and $\gamma(x) \in K_h$ for all $x \in \mathcal{C}_h$.

Remark 2. In Definition 1 there must exist a class $\mathcal{K}$ function α satisfying $\sup_{u \in U}[L_f h(x) + L_g h(x) + \alpha(h(x))] \geq 0$ which implies that an α must also be found to specify a valid ZCBF. The above result holds for all α, resolving this ambiguity.

Remark 3. The intuitive reason why h is a ZCBF is that whenever $h(x)$ is non-negative, we have by definition a control input γ available to keep the system safe. A geometric view is presented in Figure 1. Note that γ is not the output of the Quadratic Program (6). Instead, the role of γ is to allow h to be evaluated via (9).

C. Deriving a Barrier Certificate for UAV Collision Avoidance

We now consider how to calculate h defined in (9) for the UAV collision avoidance problem. From Theorem 3 the only restriction on γ and ρ is that γ is locally Lipschitz and that h is continuously differentiable so there is some flexibility in choosing γ and ρ. In this section we discuss two cases where we can choose γ and ρ so that h can be calculated in closed form. Let the initial state for vehicle i ($i = 1, 2$) be given by $\begin{bmatrix} p_{i,x_0} & p_{i,y_0} & \theta_{i,0} \end{bmatrix}^T$.

Example 1. In the first case, let

$$
\rho(x) = d_{1,2}(x) - \delta + \delta\cos(\theta_1) - D_s^2, \tag{13}
$$

where $\delta > 0$ is introduced to (8) so that h will be continuously differentiable. Let

$$\gamma_{turn} = \begin{bmatrix}\sigma v & \omega & v & \omega\end{bmatrix}^T \tag{14}$$

with $\sigma \neq 0$, $\omega \neq 0$. In other words, γ_{turn} is defined by the same turn rate for both vehicles but possibly different translational velocities. Letting $b_{1,0} = p_{1,x_0} - \sigma\frac{v}{\omega}\sin(\theta_{1,0})$, $b_{2,0} = p_{2,x_0} - \frac{v}{\omega}\sin(\theta_{2,0})$, $c_{1,0} = p_{1,y_0} + \sigma\frac{v}{\omega}\cos(\theta_{i,0})$, $c_{2,0} = p_{2,y_0} + \frac{v}{\omega}\cos(\theta_{2,0})$, $\Delta b_0 = b_{1,0} - b_{2,0}$, and $\Delta c_0 = c_{1,0} - c_{2,0}$,

$$\begin{aligned} h(x) = \\ &\inf_{\tau\in[0,\infty)} \left(\Delta b_0 + \sigma\frac{v}{\omega}\sin(\omega\tau + \theta_{1,0}) - \frac{v}{\omega}\sin(\omega\tau + \theta_{2,0})\right)\right)^2 \\ &+ \left(\Delta c_0 - \sigma\frac{v}{\omega}\cos(\omega\tau + \theta_{1,0}) + \frac{v}{\omega}\cos(\omega\tau + \theta_{2,0})\right)^2 \\ &-\delta + \delta\cos(\omega\tau + \theta_{1,0}) - D_s^2. \end{aligned}$$

By expanding the square terms and applying two trigonometric identities,[1] we get

$$\begin{aligned} h(x) = \\ &\inf_{\tau\in[0,\infty)} \Delta b_0^2 + \Delta c_0^2 + (1+\sigma^2)\frac{v^2}{\omega^2} - 2\sigma\frac{v^2}{\omega^2}\cos(\theta_{1,0} - \theta_{2,0}) \\ &+2\sigma\Delta b_0\frac{v}{\omega}\sin(\omega\tau + \theta_{1,0}) - 2\Delta b_0\frac{v}{\omega}\sin(\omega\tau + \theta_{2,0}) \\ &-2\sigma\Delta c_0\frac{v}{\omega}\cos(\omega\tau + \theta_{1,0}) + 2\Delta c_0\frac{v}{\omega}\cos(\omega\tau + \theta_{2,0}) \\ &-\delta + \delta\cos(\omega\tau + \theta_{1,0}) - D_s^2. \end{aligned}$$

Grouping constant terms and applying phasor addition yields

$$h(x) = \inf_{\tau\in[0,\infty)} A_1 + A_2\cos(\omega\tau + \Theta) - D_s^2,$$

where A_1 results from grouping constant terms, while A_2 and Θ are the amplitude and phase resulting from the phasor addition. Then in this case $h(x) = A_1 - A_2 - D_s^2$. Note that for the case where

$$\rho(x) = \sqrt{d_{1,2}(x) - \delta + \delta\cos(\theta_1)} - D_s, \tag{15}$$

the same reasoning yields $h(x) = \sqrt{A_1 - A_2} - D_s$ for ρ defined in (15). Note that $A_1 - A_2 \geq 0$ provided that the vehicles do not get more than 2δ from each other along the trajectory defined by (10) using γ_{turn} in (14).

Example 2. For a second case where we can solve (9) in closed form, let ρ be given in (8) and

$$\gamma_{straight} = \begin{bmatrix}v_1 & 0 & v_2 & 0\end{bmatrix}^T, \tag{16}$$

where $v_1 \neq v_2$. In other words, $\gamma_{straight}$ uses a 0 turn rate while allowing the vehicles to have different speeds. In this case we have

$$\begin{aligned} h(x) = \\ &\inf_{\tau\in[0,\infty)} (p_{a,x_0} + tv_1\cos(\theta_{a,0}) - p_{b,x_0} - tv_2\cos(\theta_{b,0}))^2 \\ &+ (p_{a,y_0} + tv_1\sin(\theta_{a,0}) - p_{b,y_0} - tv_2\sin(\theta_{b,0}))^2 - D_s^2, \end{aligned}$$

which is quadratic in t so the minimum can be calculated in closed form.

[1] The identities are $\sin^2(\alpha) + \cos^2(\alpha) = 1$ and $\cos(\alpha - \beta) = \cos(\alpha)\cos(\beta) + \sin(\alpha)\sin(\beta)$.

D. Simulation of Two Vehicles

We demonstrate the theoretical development of this section in simulation using SCRIMMAGE [36]. SCRIMMAGE is a multi-agent simulator designed to scale to high numbers of vehicles and includes a plugin-interface that makes it easy to experiment with different motion models and controllers without having to change code. This makes it simple to swap out nominal controllers and vary the fidelity of fixed-wing UAVs from the unicycle dynamics in (2) used in this section up to a 6-DOF model.

For the simulation, let k vehicles be positioned in a circle of radius 200 around the origin, where $k = 2$ in this simulation. In other words, vehicle i has initial state $x_i = \begin{bmatrix}200\cos\left(i\frac{2\pi}{k} + \pi\right) & 200\sin\left(i\frac{2\pi}{k} + \pi\right) & i\frac{2\pi}{k} + \psi\end{bmatrix}^T$, where ψ is an additional offset so that vehicles are not necessarily starting with orientation pointing at the origin. The goal position for vehicle i is on the other side of the origin: $x_{i,g} = \begin{bmatrix}200\cos\left(i\frac{2\pi}{k}\right) & 200\sin\left(i\frac{2\pi}{k}\pi\right)\end{bmatrix}^T$.

This setup is selected so that the vehicles are on a collision course. The nominal controller is that described in [37] with constant $\lambda = 1$. Additionally, we let $v_{min} = 15$ meters/second, $v_{max} = 25$ meters/second, $\omega_{max} = 13$ degrees/second, $D_s = 5$ meters, and $\delta = 0.01$ meters^2. ω_{max} is chosen to be consistent with a constant rate turn [38] with a 30 degree bank with a speed of v_{max}. Each vehicle evaluates (6) at each timestep where we use OSCP [39] to evaluate the QP. We investigate the performance of the vehicles when h defined in (9) is constructed from γ_{turn} in (14) and $\gamma_{straight}$ (17), respectively, where $\gamma_{turn} = \begin{bmatrix}1.1v & \omega & v & \omega\end{bmatrix}^T$, $\gamma_{straight} = \begin{bmatrix}1.1v & 0 & v & 0\end{bmatrix}^T$, and $v = 0.9v_{min} + 0.1v_{max}$ and $\omega = 0.9\omega_{max}$. For the scenario with γ_{turn}, we let $\psi = 0$ so that the vehicles start with orientation pointing at the origin. For the scenario with $\gamma_{straight}$, we let $\psi = 2°$ because if the vehicles pointed at the origin they would not start in the safe set. Additionally, for the γ_{turn} case we use ρ in (15). Similarly, for the $\gamma_{straight}$ case we use $\rho(x) = \sqrt{d_{1,2}(x)} - D_s$. Details of the distance between the vehicles and control signals are shown in Figure 2. Note that the resulting trajectory can be different depending on which γ is used as shown in Figure 2d. Nevertheless, in both cases the vehicles are able to maintain safe distances from each other and satisfy actuator constraints throughout the simulation regardless of which γ is used to construct a h.

IV. COMPOSITION OF MULTIPLE SAFETY CONSTRAINTS

A. Motivating Example

Although the constructive method introduced in (9) can produce a barrier certificate in the presence of actuator constraints that ensures two vehicles do not collide, the formulation does not extend immediately to collision avoidance for systems with more than two vehicles. To see this, we present a specific example where three UAVs with a collision avoidance safety objective cannot use the results from Section III-B to ensure safety. A plot of this scenario is shown in Figure 3. We index the vehicles by $i = 1, 2, 3$. To ensure collision-free trajectories,

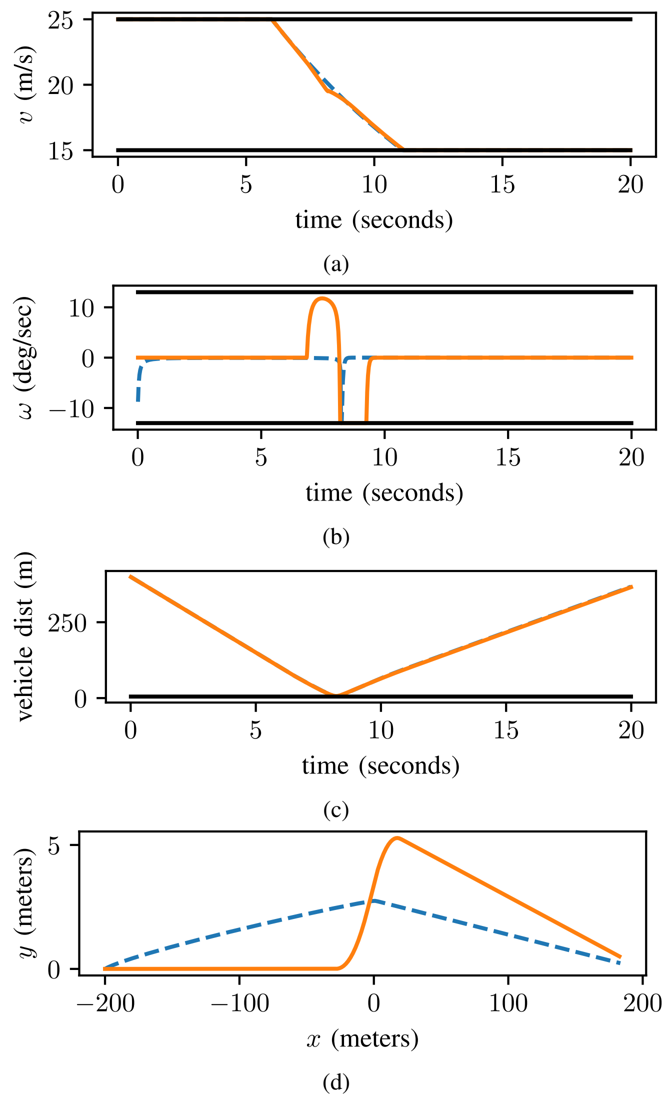

Fig. 2: Outputs for the scenario with 2 fixed-wing vehicles. The blue dashed and orange solid lines are the output of the scenario where h is constructed from $\gamma_{straight}$ and γ_{turn}, respectively. Vehicle 1 velocity and turn rates are shown to be within the actuator limits in (a) and (b). The minimum distance between the vehicles is shown to be above D_s in (c) where the output is very similar in both scenarios. The path taken by vehicle 1 is shown in (d). Note that the choice of γ in constructing h has a significant effect on the path taken.

and considering the safety function defined in (13), three pairwise constraints must be nonnegative at all times:

$$\begin{aligned}\rho^1(x) &= d_{1,2}(x) - \delta + \delta\cos(\theta_1) - D_s^2,\\ \rho^2(x) &= d_{1,3}(x) - \delta + \delta\cos(\theta_1) - D_s^2,\\ \rho^3(x) &= d_{2,3}(x) - \delta + \delta\cos(\theta_2) - D_s^2.\end{aligned}$$

We now apply these results of Section III to these constraints and for simplicity, let δ be approximately 0. For each constraint, define an arbitrarily chosen nominal evading maneuver

$$\gamma^1(x) = \begin{bmatrix}1 & -1 & 1 & -1 & 1 & -1\end{bmatrix}^T \tag{16a}$$

$$\gamma^2(x) = \gamma^3(x) = \begin{bmatrix}1 & 1 & 1 & 1 & 1 & 1\end{bmatrix}^T. \tag{16b}$$

In other words, γ^1 encodes an evasive maneuver where all the vehicles turn right while γ^2 and γ^3 encode a maneuver where all the vehicles turn left. We note that h^j $(j = 1, \dots, 3)$ defined in (9) and constructed from ρ^j and γ^j are ZCBFs. In this example we let $v_{min} = 1$, $v_{max} = 2$, $\omega_{max} = 1$, and $D_s = 0.5$ so that the vehicles follow a circular trajectory with radius $r = 1$ when applying v_{min} and ω_{max}. Assume now that the vehicles have the following initial states

$$\begin{aligned}x_1 &= \begin{bmatrix}0 & 0 & 0\end{bmatrix}^T,\\ x_2 &= \begin{bmatrix}(2r + D_s)\sin\psi & (2r + D_s)\cos\psi - 2r & \pi\end{bmatrix}^T,\\ x_3 &= \begin{bmatrix}(2r + D_s)\sin\psi & 2r - (2r + D_s)\cos\psi & \pi\end{bmatrix}^T,\end{aligned}$$

where $\psi = \arccos\left(\frac{D_s/2 + 2r}{2r + D_s}\right)$. Then $h^1(x) = h^2(x) = h^3(x) = 0$ and the barrier constraints in (4) for $h^1(x)$ and $h^2(x)$ become

$$-0.4(v_1 + \omega_1 + v_2 + \omega_2) \geq 0 \tag{17}$$

$$0.4(-v_1 + \omega_1 - v_3 + \omega_3) \geq 0. \tag{18}$$

Although h^1 and h^2 are ZCBFs, these two constraints cannot be simultaneously satisfied for $v_i \in [v_{min}, v_{max}]$ and $|\omega_i| \leq \omega_{max}$. In particular, after substituting the minimum velocity $v_1 = v_2 = 1$, the first equation dictates that $\omega_1 + \omega_2 \leq -2$ (i.e., vehicles 1 and 2 must turn right). Similarly, the second equation dictates that vehicle 1 and 3 must turn left. The problem with this scenario is that vehicle 1 cannot simultaneously execute both nominal evading maneuvers (i.e., turn both left and right at the same time). To solve this problem, we will make sure that the evasive maneuver applied by a vehicle is the same for every barrier certificate. A geometric view of the general problem and its solution are shown in Figure 4.

B. Problem Statement For Satisfying Multiple Objectives

In order to solve the issues arising when vehicles have to simultaneously respect multiple constraints, we now extend the use of the constructive technique introduced in (9). Suppose there are q constraints $\rho^j : \mathcal{D} \to \mathbb{R}$ $(j = 1, \dots, q)$ that must be greater than or equal to 0 at all times. For the k agents with pairwise constraints $q = k(k-1)/2$. We assume that for each constraint $j = 1, \dots, q$, a locally Lipschitz nominal evading maneuver γ^j has been selected using the framework in (9). An example for fixed-wing UAVs with collision avoidance safety constraints is given in (14). We assume h^j is constructed according to (9) and is continuously differentiable so that h^j is a ZCBF for $j = 1, \dots, q$. Denote the overall safe set and overall admissible control space as

$$C_\cap = C_{h^1} \cap \dots \cap C_{h^q}, \tag{19}$$

$$K_\cap(x) = \{u \in U \ : \ u \in K_{h^1}(x) \cap K_{h^2}(x) \cap \dots \cap K_{h^q}(x)\}.$$

Lemma 1. *Suppose h^j is a ZCBF for $j = 1, \dots, q$. Then any Lipschitz continuous controller $u : \mathcal{C}_h \to U$ such that $u(x) \in K_\cap(x)$ will render the set $C_\cap$ forward invariant.*

Proof. Suppose $x \in C_\cap$. Then $x \in C_{h^j}$ for $j = 1, \dots, q$. Because $u \in K_\cap$, $u \in K_{h^j}$ for $j = 1, \dots, q$, so it follows from Theorem 1 that C_{h^j} is forward invariant. In other words, if $x(0) \in C_\cap$ then $x(t) \in C_{h^j}$ for all $t \geq 0$ for $j = 1, \dots, q$.

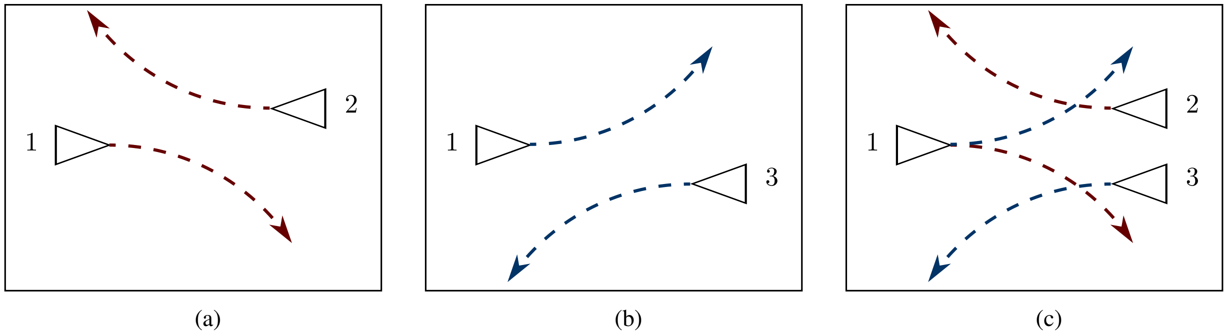

Fig. 3: A geometric view of the example given in Section IV-A. In (a), h^1 defined in (9) is constructed to design a certificate so that vehicles 1 and 2 stay safe. Here γ^1 encodes an evasive maneuver where vehicles 1 and 2 turn right. Further, vehicles 1 and 2 are placed so that turning right is the only available control input to keep the system safe. In (b), a similar setup is shown for vehicles 1 and 3 where h^2 has been constructed from γ^2 which enodes an evasive manuever where vehicles 1 and 3 turn left and vehicles 1 and 3 placed so they are only able to turn left to stay safe. In (c), vehicle 1 cannot turn both right and left to avoid vehicles 2 and 3, respectively. Although vehicle 1 can avoid them individually, it cannot avoid them both simultaneously.

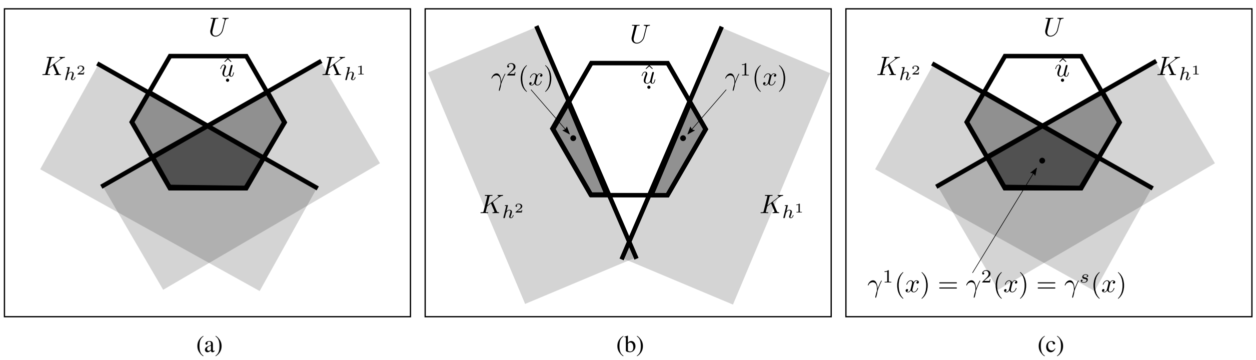

Fig. 4: A geometric view of why having a set of individual barrier certificates does not guarantee that a control input u exists to satisfy each associated constraint and how the shared evading maneuver assumption resolves this issue. In (a), multiple barrier function constraints are shown as half-spaces. To satisfy Lemma 1, a u must be selected that is in the intersection of K_{h^1}, K_{h^2}, and U. In (b), although there exists a u that is in the intersection of U and K_{h^1} as well as U and K_{h^2}, as guaranteed by the fact that h^1 and h^2 are ZCBFs, there does not exist a u that is in the intersection of U, K_{h^1}, and K_{h^2}. This case corresponds to the specific scenario for the three vehicle collision avoidance problem in Fig. 3c. In (c), the problem is resolved by the shared evading maneuver because $\gamma^s(x)$ satisfies each constraint.

Therefore if $x(0) \in C_\cap$ then $x(t) \in C_\cap$ for all $t \geq 0$ so $C_\cap$ is forward invariant. $\square$

C. The Shared Nominal Evading Maneuver Assumption

Section IV-A showed an example where $K_\cap$ could be empty for some $x \in \mathcal{C}_\cap$. As a result, the assumptions of Lemma 1 could not be satisfied. In order to address the issue discussed in Section IV-A, we introduce an additional constraint on γ^j ($j = 1, \dots, q$) that all h^j are constructed from the same nominal evading maneuver.

Definition 2. Suppose every h^j ($j = 1, \dots, q$) is defined as in (9) and is constructed from γ^j, respectively. The *shared evading maneuver assumption* holds if $\gamma^1(x) = \cdots = \gamma^q(x)$ for all $x \in \mathcal{D}$. The *shared evading maneuver* is denoted γ^s so that $\gamma^s(x) = \gamma^1(x) = \cdots = \gamma^q(x)$ for all $x \in \mathcal{D}$.

Remark 4. This assumption requires that each h^j ($j = 1, \dots, q$) be constructed from the same nominal evading maneuver. Note, however, that this does not imply that each h^j must be constructed from the same safety function ρ^j.

The example in Section IV-A does not satisfy the shared evading maneuver assumption because $\gamma^1(x)$ and $\gamma^2(x)$ defined in (17) are not the same. To enforce that the shared evasive maneuver assumption holds, one option is to change γ^1 so that

$$\gamma^1(x) = \begin{bmatrix} 1 & 1 & 1 & 1 & 1 & 1 \end{bmatrix}^T. \tag{20}$$

In other words, using γ^1 defined in (20) and γ^2 and γ^3 in (16b) implies an evasive maneuver where all vehicles turn left for each constraint. Another example where the shared nominal evading maneuver assumption holds is as follows:

$$\gamma^s(x) = \gamma^1(x) = \gamma^2(x) = \gamma^3(x) = \begin{bmatrix}1 & 1 & 1.5 & 0 & 2 & -1\end{bmatrix}^T.$$

In this case, $\gamma^s(x)$ encodes an evasive maneuver where vehicle 1 turns left with a linear velocity of 1, vehicle 2 stays straight with a linear velocity of 1.5, and vehicle 3 turns right with a linear velocity of 2. These three nominal evading maneuvers satisfy the shared evasive maneuver assumption because for all $x \in \mathcal{D}$, $\gamma^1(x) = \gamma^2(x) = \gamma^3(x)$.

To see the purpose of the shared evading maneuver assumption, we first examine the case of a single constraint. In particular, let h be defined in (9) and consider the role of γ in establishing that h is a ZCBF. From Definition 1, for h to be used for a barrier certificate, $K_h(x)$ must be nonempty for all $x \in \mathcal{D}_h$. With h defined as in (9), this property is satisfied by $\gamma(x)$ for all $x \in \mathcal{C}_h$ (see Theorem 3). The analogue condition for multiple constraints is that $K_\cap(x)$ is non-empty for all $x \in \mathcal{C}_\cap$. If each h^j defined in (9) is a ZCBF and is constructed from γ^j then by similar reasoning to Theorem 3, $\gamma^j(x) \in K_{h^j}(x)$ for all $x \in \mathcal{C}_{h^j}$. If $\gamma^1(x) = \cdots = \gamma^j(x)$ for all $x \in \mathcal{C}_\cap$ then we can additionally conclude that $K_\cap(x)$ is non-empty for all $x \in \mathcal{C}_{h^j}$.

D. Calculating a Safe Control Law

With the shared evading maneuver assumption, we can calculate $u \in K_\cap$ so that u is Lipschitz continuous. To do so, we write the QP in (6) with q constraints and let $\hat{u} = \begin{bmatrix}\hat{u}_1^T & \hat{u}_2^T & \cdots & \hat{u}_k^T\end{bmatrix}^T$ where $\hat{u}_i$ is the nominal input of vehicle i for $i = 1, \dots, k$. To emphasize that all h^j are constructed from γ^s, we write $h^j(x;\rho^j,\gamma^s)$ for each $j = 1, \dots, q$.

$$\begin{aligned} u^* = \min_{u \in \mathbb{R}^m} \ & \frac{1}{2}\|u - \hat{u}\|^2 \qquad (21)\\ \text{s.t.} \quad & Au \geq b. \\ & L_f h^j(x;\rho^j,\gamma^s) + L_g h^j(x;\rho^j,\gamma^s)u \\ & \quad +\alpha(h^j(x;\rho^j,\gamma^s)) \geq 0 \qquad j \in \{1,\dots,q\} \end{aligned}$$

Theorem 4. *Suppose $C_\cap$ is defined as in (19) where h^j ($j = 1, \dots, q$) defined in (9) is continuously differentiable and the shared evading maneuver assumption holds. In addition, suppose that h^j has a Lipschitz continuous derivative for $j = 1, \dots, q$, $\hat{u}$ and γ^s are Lipschitz continuous, γ^s maps to the interior of U, and that x is in the interior of $\mathcal{C}_\cap$. Then u^* in (21) is Lipschitz continuous and $\mathcal{C}_\cap$ is forward invariant.*

Proof. Under these assumptions γ^s is strictly feasible so u^* is Lipschitz continuous as an application of Theorem 1 of [40]. $\mathcal{C}_\cap$ is then forward invariant by Lemma 1. □

Theorem 4 gives conditions for ensuring that for all $x \in \mathcal{C}_\cap$, a Lipschitz continuous $u \in K_\cap(x)$ can be calculated, thus resolving the issue presented in Section IV-A. A geometric view of the problem and resolution is shown in Figure 4.

V. DECENTRALIZED CONTROL CALCULATION

The QP in (21) is a centralized calculation. In particular, it requires that each vehicle's nominal control input $\hat{u}_i$ be communicated. Frequently communicating this signal when there are many vehicles may reduce throughput for other important messages or introduce communication delays. Thus, we show how to ensure safety constraints can be satisfied by reformulating the QP so that the vehicles can calculate a safe control signal without requiring each other's nominal control input.

Let $\gamma^s = \begin{bmatrix}\gamma_1^{s^T} & \cdots & \gamma_k^{s^T}\end{bmatrix}^T$, where γ_i^s maps to vectors of the same size as u_i for $i = 1, \dots, k$ with similar decomposition for $b = \begin{bmatrix}b_1^T & \cdots & b_k^T\end{bmatrix}^T$ and $L_g h^j(x;\rho^j;\gamma^s) = \begin{bmatrix}[L_g h^j(x;\rho^j;\gamma^s)]_1^T & \cdots & [L_g h^j(x;\rho^j;\gamma^s)]_k^T\end{bmatrix}^T$. Further, assume A in (6c) is block diagonal with block entries A_i for $i = 1, \dots, k$ where A_i is a $m_i \times m_i$ matrix. This assumption means that actuator constraints are not coupled between vehicles. For constraint j for $j = 1, \dots, q$, let

$$\zeta^j = \{i \in \{1,\dots,k\} : \exists x \in \mathcal{D} \text{ s.t. } [L_g h^j(x;\rho^j,\gamma^s)]_i \neq 0_{m_i}\}$$

where 0_{m_i} is the zero vector in $\mathbb{R}^{m_i}$. ζ^j represents the set of vehicles whose control input affects the time derivative of h^j for some $x \in \mathcal{D}$. We let $|\zeta^j|$ denote the cardinality of ζ^j, and note that for the case of pairwise collision avoidance, $|\zeta^j| = 2$ for all $j = 1, \dots, q$. In the example with three vehicles in Section IV, $\zeta_1 = \{1,2\}$, $\zeta_2 = \{1,3\}$, $\zeta_3 = \{2,3\}$. Finally, we denote $u_{\setminus i} = \begin{bmatrix}u_1^T & \cdots & u_{i-1}^T & u_{i+1}^T & \cdots & u_k^T\end{bmatrix}^T$, with similar definitions for $\gamma_{\setminus i}^s$, $\hat{u}_{\setminus i}$, and $[L_g h^j(x;\rho^j;\gamma^s)]_{\setminus i}$.

With the above definitions, we can now state a decentralized analogue for the admissible control space in (5). The decentralized admissible control space for constraint j ($j = 1, \dots, q$) and vehicle i ($i \in \zeta^j$) is defined as

$$\begin{aligned} \mathcal{K}_{i,j}(x) = \{u_i \in U_i \ : \ & \\ & L_f h^j(x;\rho^j,\gamma^s) + [L_g h^j(x;\rho^j,\gamma^s)]_i u_i + \alpha(h^j(x;\rho^j,\gamma^s)) \\ & +[L_g h^j(x;\rho^j,\gamma^s)]_{\setminus i}\gamma_{\setminus i}^s(x) \\ & -\frac{|\zeta^j|-1}{|\zeta^j|}\Big(L_f h^j(x;\rho^j,\gamma^s) + L_g h^j(x;\rho^j,\gamma^s)\gamma^s(x) \\ & \qquad +\alpha(h^j(x;\rho^j,\gamma^s))\Big) \geq 0\}. \end{aligned}$$

Let $\mathcal{A}_i = \{j \in \{1,\dots,q\} \ : \ i \in \zeta^j\}$ so that $\mathcal{A}_i$ is the set of indices where u_i has an effect on the time derivative of the associated barrier certificate for some $x \in \mathcal{D}$. For the three vehicle example of Section IV, $\mathcal{A}_1 = \{1,2\}$, $\mathcal{A}_2 = \{1,3\}$, $\mathcal{A}_3 = \{2,3\}$. The decentralized admissible control space for vehicle i is then $\mathcal{K}_i(x) = \bigcap_{l \in \mathcal{A}_i} \mathcal{K}_{i,l}$ and the overall decentralized admissible control space is

$$\mathcal{K}(x) = \{u = \begin{bmatrix}u_1^T & \cdots & u_k^T\end{bmatrix}^T \in U \ : \ u_i \in \mathcal{K}_i(x) \ \forall i \in \{1,\dots,k\}\}.$$

Theorem 5. *Suppose $C_\cap$ is defined as in (19) where h^j is continuously differentiable and the shared evading maneuver assumption holds where γ^s is locally Lipschitz. Then $\forall x \in \mathcal{C}_\cap$, $\gamma^s \in \mathcal{K}(x)$ and $\mathcal{K}(x) \subseteq K_\cap(x)$.*

Proof. Consider the first statement, namely that $\gamma^s \in \mathcal{K}(x)$. For $j = 1, \dots, q$, consider any $i \in \zeta^j$ and let $u_i = \gamma_i^s$. Then

$$\begin{aligned} &L_f h^j(x;\rho^j,\gamma^s) + [L_g h^j(x;\rho^j,\gamma^s)]_i u_i + \alpha(h^j(x;\rho^j,\gamma^s)) \\ &\quad + [L_g h^j(x;\rho^j,\gamma^s)]_{\setminus i}\gamma^s_{\setminus i}(x) \\ &\quad - \frac{|\zeta^j|-1}{|\zeta^j|}\Big(L_f h^j(x;\rho^j,\gamma^s) + L_g h^j(x;\rho^j,\gamma^s)\gamma^s(x) \\ &\qquad + \alpha(h^j(x;\rho^j,\gamma^s))\Big) \\ &= \frac{1}{|\zeta^j|}(L_f h^j(x) + L_g h^j(x)\gamma^s(x) + \alpha(h^j(x))) \geq 0. \end{aligned}$$

The inequality is true because $x \in \mathcal{C}_\cap$ implies $\alpha(h^j(x;\rho^j,\gamma^s)) \geq 0$. See the proof for Theorem 3 for why $L_f h^j(x;\rho^j,\gamma^s) + L_g h^j(x;\rho^j,\gamma^s)\gamma^s(x) \geq 0$. Then $\gamma_i^s \in \mathcal{K}_{i,j}$ for any $j = 1, \dots, q$ and $i \in \zeta^j$. Then $\gamma_i^s \in \mathcal{K}_i$. Then $\gamma^s(x) \in \mathcal{K}(x)$.

For the second statement, assume $u \in \mathcal{K}(x)$ so that $u_i \in \mathcal{K}_i(x)\ \forall i \in \{1, \dots, k\}$. This means that $A_i u_i \geq b_i$ so that, because A is block diagonal, $Au \geq b$. Further, it means that for any constraint $j = 1, \dots, q$ and any $i \in \zeta^j$,

$$\begin{aligned} &L_f h^j(x;\rho^j,\gamma^s) + [L_g h^j(x;\rho^j,\gamma^s)]_i u_i + \alpha(h^j(x;\rho^j,\gamma^s)) \\ &\quad + [L_g h^j(x;\rho^j,\gamma^s)]_{\setminus i}\gamma^s_{\setminus i}(x) \\ &\quad - \frac{|\zeta^j|-1}{|\zeta^j|}\Big(L_f h^j(x;\rho^j,\gamma^s) + L_g h^j(x;\rho^j,\gamma^s)\gamma^s(x) \\ &\qquad + \alpha(h^j(x;\rho^j,\gamma^s))\Big) \geq 0. \end{aligned} \tag{22}$$

To simplify (22), note that by definition, $[L_g h(x)]_i = 0$ for $i \neq \zeta^j$ so that

$$\begin{aligned} \sum_{i\in\zeta^j}[L_g h^j(x;\rho^j;\gamma^s)]_i u_i &= \sum_{i\in\{1,\dots,k\}}[L_g h^j(x;\rho^j;\gamma^s)]_i u_i \\ &= L_g h^j(x;\rho^j;\gamma^s)u. \end{aligned} \tag{23}$$

Using (23) in the following then yields

$$\begin{aligned} &\sum_{i\in\zeta^j}[L_g h^j(x;\rho^j,\gamma^s)]_{\setminus i}\gamma^s_{\setminus i}(x) \\ &= \sum_{i\in\zeta^j}\big(L_g h^j(x;\rho^j,\gamma^s)\gamma^s(x) - [L_g h^j(x;\rho^j,\gamma^s)]_i\gamma_i^s(x)\big) \\ &= |\zeta^j| L_g h^j(x;\rho^j,\gamma^s)\gamma^s(x) - \sum_{i\in\zeta^j}[L_g h^j(x;\rho^j,\gamma^s)]_i\gamma_i^s(x) \\ &= |\zeta^j| L_g h^j(x;\rho^j,\gamma^s)\gamma^s(x) - L_g h^j(x;\rho^j,\gamma^s)\gamma^s(x) \\ &= (|\zeta^j|-1)L_g h^j(x;\rho^j,\gamma^s)\gamma^s(x). \end{aligned} \tag{24}$$

Summing (22) over $i \in \zeta^j$ and using (23) and (24) yields

$$\begin{aligned} 0 \leq\ &|\zeta^j| L_f h^j(x;\rho^j,\gamma^s) + L_g h^j(x;\rho^j,\gamma^s)u \\ &+ |\zeta^j|\alpha(h^j(x;\rho^j,\gamma^s)) + (|\zeta^j|-1)L_g h^j(x;\rho^j,\gamma^s)\gamma^s(x) \\ &- (|\zeta^j|-1)\Big(L_f h^j(x;\rho^j,\gamma^s) + L_g h^j(x;\rho^j,\gamma^s)\gamma^s(x) \\ &\qquad + \alpha(h^j(x;\rho^j,\gamma^s))\Big) \\ =\ &L_f h^j(x;\rho^s,\gamma^s) + L_g h^j(x;\rho^s,\gamma^s)u + \alpha(h^j(x;\rho^s,\gamma^s)). \end{aligned}$$

Since this is true for all $j = 1, \dots, q$, $u \in K_\cap(x)$. Then $\mathcal{K}(x) \subseteq K_\cap(x)$ for all $x \in \mathcal{C}_\cap$. □

In particular, Theorem 5 implies that when vehicle i (for all $i \in \{1, \dots, k\}$) calculates the following QP, the QP will be feasible for all $x \in \mathcal{C}_\cap$, and $\mathcal{C}_\cap$ will be forward invariant:

$$\begin{aligned} u_i^* = &\min_{u_i\in\mathbb{R}^{m_i}} \frac{1}{2}\|u_i - \hat{u}_i\|^2 \\ \text{s.t.}\quad &A_i u_i \geq b_i \\ &L_f h^j(x;\rho^j,\gamma^s) + [L_g h^j(x;\rho^j,\gamma^s)]_i u_i \\ &\quad + \alpha(h^j(x;\rho^j,\gamma^s)) + [L_g h^j(x;\rho^j,\gamma^s)]_{\setminus i}\gamma^s_{\setminus i}(x) \\ &\quad - \frac{|\zeta^j|-1}{|\zeta^j|}\Big(L_f h^j(x;\rho^j,\gamma^s) + L_g h^j(x;\rho^j,\gamma^s)\gamma^s(x) \\ &\qquad + \alpha(h^j(x;\rho^j,\gamma^s))\Big) \qquad j \in \mathcal{A}_i \end{aligned} \tag{25}$$

Theorem 6. *Under the same assumptions of Theorem 4, u_i^* in (25) is Lipschitz continuous and $\mathcal{C}_\cap$ is forward invariant.*

Proof. γ_i^s is strictly feasible so u_i^* is Lipschitz continuous as an application of Theorem 1 of [40]. Then $u = \begin{bmatrix} u_1^* & \cdots u_k^* \end{bmatrix}^T$ is Lipschitz continuous and because $u_i^* \in \mathcal{K}_i(x)$, $u \in \mathcal{K}(x)$. Then by Theorem 5, $u \in K_\cap(x)$ and $\mathcal{C}_\cap$ is forward invariant by Lemma 1. □

We note that the solution from the centralized QP (21) may be different than the solution from the decentralized QPs (25) because $\mathcal{K}(x)$ may be a strict subset of $K_\cap(x)$. To see this, let $k = 2$, $q = 1$, $L_f h(x) = 0$, $\alpha(h(x)) = 0$, $m_1 = m_2 = 1$, $[L_g h(x)]_2\gamma_2^s(x) = -1$, and $[L_g h(x)]_1\gamma_1^s(x) = 1$. Then the barrier certificate constraint in (25) becomes $[L_g h(x)]_1 u_1 \geq 1$, while the barrier certificate constraint in (21) becomes $L_g h(x)u \geq 0$. Since $u_1 = 0$ is feasible for the latter but not the former equation, we do not have that $\mathcal{K}(x) = K_\cap(x)$. Although the decentralized QP (25) can be used to ensure safety by Theorem 6, because $\mathcal{K}(x) \subset K_\cap(x)$, it may be that the total cost of each vehicle calculating (25) is higher than the centralized calculation (21). In other words, the calculated safe control may not be as close to the nominal control signal in a least squares sense when using (25) as opposed to (21).

Another difference between the decentralized (25) and the centralized (21) QPs is how the size of the optimization variable and number of constraints vary with the number of vehicles k. In the centralized approach (21) the size of the optimization variable grows linearly with k while the number of constraints grows quadratically. On the other hand, in the decentralized QP (25), the size of the optimization variable and number of constraints are constant and linear, respectively.

VI. SIMULATION

In this section we repeat the scenario discussed in Section III-D but consider $k = 20$ vehicles. For the scenario where h is constructed from γ_{turn}, we use $\begin{bmatrix} v & \omega & v & \omega \end{bmatrix}^T$ where $v = 0.9v_{min} + 0.1v_{max}$ and $\omega = 0.9\omega_{max}$. For the scenario where h is constructed from $\gamma_{straight}$, we let $\gamma^i = \begin{bmatrix} (1 + 0.01i)v & 0 \end{bmatrix}^T$ so that each vehicle uses a different translational velocity as is required to ensure differentiability of h (see Section III-C). Note that this does not violate the shared evading maneuver assumption because $\gamma^s = \begin{bmatrix} (\gamma^1)^T & \cdots & (\gamma^k)^T \end{bmatrix}^T$. Additionally, we let $\psi = 0$ and $\psi = 25°$ in the scenario where h is constructed from γ_{turn} and

$\gamma_{straight}$, respectively. Offsetting the initial orientation $25°$ from pointing at the origin is required so that the vehicles can start in the safe set when using $\gamma_{straight}$. Screenshots for the case of γ_{turn} and $\gamma_{straight}$ are shown in Figures 5 and 6, respectively. Quantitative results for both scenarios are shown in Figure 7 which shows similar outputs to the results for the two vehicle simulation shown in Figure 2. In particular, the pairwise distance between all vehicles are kept above the minimum safety distance D_s while satisfying actuator constraints.

VII. Conclusion

In this paper we have examined how to ensure that for vehicles characterized by constrained inputs, multiple barrier certificates can be satisfied simultaneously while relaxing communication requirements. The resulting solution is a decentralized algorithm that was applied to a collision avoidance scenario with fixed-wing UAVs where in spite of communication restrictions, the vehicles are able to maintain safe distances from each other.

Appendix A
Proof for Theorem 2

Proof. Starting from the definition of the derivative of h from (9), we expand terms using a Taylor series and simplify the expression using an argument by contradiction. Let ν_k be a sequence in $\mathbb{R}^n$ approaching zero, $\hat{x} + \delta x_k$ be the trajectory starting from $x(t) + \nu_k$ rather than $x(t)$, $\frac{\partial \hat{x}(t+\tau)}{\partial x(t)}$ the derivative of the solution at time $t+\tau$ with respect to initial conditions, and $\tau_1 \geq 0$ a time for which $\rho(\hat{x}(t+\tau))$ is a minimum. Note that $\frac{\partial \hat{x}(t+\tau)}{\partial x(t)}$ is well defined by Theorem 6.1 of [41] and noting that $\dot{\hat{x}}$ is continuously differentiable. We start with the following:

$$\lim_{k\to\infty} \frac{h(x(t)+\nu_k) - h(x(t))}{\|\nu_k\|} = \lim_{k\to\infty} \frac{\inf_{\tau\in[0,\infty)} \rho((\hat{x}+\delta x_k)(t+\tau)) - \inf_{\tau\in[0,\infty)} \rho(\hat{x}(t+\tau_1))}{\|\nu_k\|}. \tag{26}$$

We claim that as k approaches ∞,

$$\rho(\hat{x}(t+\tau_1)) + \frac{\partial \rho(\hat{x}(t+\tau_1))}{\partial \hat{x}(t+\tau_1)} \frac{\partial \hat{x}(t+\tau_1)}{\partial x(t)} \nu_k = \inf_{\tau\in[0,\infty)} \rho((\hat{x}+\delta x_k)(t+\tau)). \tag{27}$$

Suppose not and let $\tau_{2,k} \geq 0$ be a time for which $\rho((\hat{x} + \delta x_k)(t+\tau))$ is a minimum. As a first case, suppose $\rho(\hat{x}(t+\tau_1)) + \frac{\partial \rho(\hat{x}(t+\tau_1))}{\partial \hat{x}(t+\tau_1)} \frac{\partial \hat{x}(t+\tau_1)}{\partial x(t)} \nu_k > \rho((\hat{x}+\delta x_k)(t+\tau_{2,k})) + \alpha$ for some $\alpha > 0$. Then for large enough k,

$$\begin{aligned} &\rho(\hat{x}(t+\tau_1)) + \frac{\partial \rho(\hat{x}(t+\tau_1))}{\partial \hat{x}(t+\tau_1)} \frac{\partial \hat{x}(t+\tau_1)}{\partial x(t)} \nu_k \\ &> \rho((\hat{x}+\delta x_k)(t+\tau_{2,k}) + \alpha \\ &\geq \rho(\hat{x}(t+\tau_{2,k})) + \frac{\partial \rho(\hat{x}(t+\tau_{2,k}))}{\partial \hat{x}(t+\tau_{2,k})} \frac{\partial \hat{x}(t+\tau_{2,k})}{\partial x(t)} \nu_k + \alpha/2 \\ &\geq \rho(\hat{x}(t+\tau_1)) + \frac{\partial \rho(\hat{x}(t+\tau_{2,k}))}{\partial \hat{x}(t+\tau_{2,k})} \frac{\partial \hat{x}(t+\tau_{2,k})}{\partial x(t)} \nu_k + \alpha/2. \end{aligned}$$

The last inequality holds because τ_1 is a time for which $\rho(\hat{x}(t+\tau))$ is a minimum so $\rho(\hat{x}(t+\tau_1)) \leq \rho(\hat{x}(t+\tau_{2,k}))$. Letting $k \to \infty$, we get $0 > \alpha/2$, a contradiction. In the other case, suppose $\rho(\hat{x}(t+\tau_1)) + \frac{\partial \rho(\hat{x}(t+\tau_1))}{\partial \hat{x}(t+\tau_1)} \frac{\partial \hat{x}(t+\tau_1)}{\partial x(t)} \nu_k < \rho((\hat{x}+\delta x_k)(t+\tau_{2,k})) - \alpha$ for some $\alpha > 0$. Then for large enough k,

$$\begin{aligned} \rho((\hat{x}+\delta x_k)(t+\tau_{2,k})) - \alpha/2 &> \rho((\hat{x}+\delta x_k)(t+\tau_1)) \\ &> \rho((\hat{x}+\delta x_k)(t+\tau_{2,k})). \end{aligned}$$

The second inequality holds because $\tau_{2,k}$ is a time for which $\rho((\hat{x}+\delta x_k)(t+\tau)$ is a minimum. Letting $k \to \infty$, we get $-\alpha/2 > 0$, a contradiction. Then (27) holds. From (26) and (27) we then conclude that

$$\lim_{k\to\infty} \frac{h(x(t)+\nu_k) - h(x(t))}{\|\nu_k\|} = \lim_{k\to\infty} \frac{\frac{\partial \rho(\hat{x}(t+\tau_1))}{\partial \hat{x}(t+\tau_1)} \frac{\partial \hat{x}(t+\tau_1)}{\partial x(t)} \nu_k}{\|\nu_k\|}. \tag{28}$$

In other words, $\frac{\partial h(x(t))}{\partial x(t)} = \frac{\partial \rho(\hat{x}(t+\tau_1))}{\partial \hat{x}(t+\tau_1)} \frac{\partial \hat{x}(t+\tau_1)}{\partial x(t)}$. □

References

[1] P. Kopardekar, J. Rios, T. Prevot, M. Johnson, J. Jung, and J. Robinson, "Unmanned aircraft system traffic management (utm) concept of operations," in *AIAA Aviation Forum*, 2016.

[2] S. Temizer, M. Kochenderfer, L. Kaelbling, T. Lozano-Pérez, and J. Kuchar, "Collision avoidance for unmanned aircraft using markov decision processes," in *AIAA guidance, navigation, and control conference*, 2010, p. 8040.

[3] T. B. Wolf and M. J. Kochenderfer, "Aircraft collision avoidance using monte carlo real-time belief space search," *Journal of Intelligent & Robotic Systems*, vol. 64, no. 2, pp. 277–298, 2011.

[4] D. Fox, W. Burgard, and S. Thrun, "The dynamic window approach to collision avoidance," *IEEE Robotics & Automation Magazine*, vol. 4, no. 1, pp. 23–33, 1997.

[5] M. Seder and I. Petrovic, "Dynamic window based approach to mobile robot motion control in the presence of moving obstacles," in *Robotics and Automation, 2007 IEEE International Conference on*. IEEE, 2007, pp. 1986–1991.

[6] E. Lalish, K. A. Morgansen, and T. Tsukamaki, "Decentralized reactive collision avoidance for multiple unicycle-type vehicles," in *American Control Conference, 2008*. IEEE, 2008, pp. 5055–5061.

[7] S. Mastellone, D. M. Stipanović, C. R. Graunke, K. A. Intlekofer, and M. W. Spong, "Formation control and collision avoidance for multi-agent non-holonomic systems: Theory and experiments," *The International Journal of Robotics Research*, vol. 27, no. 1, pp. 107–126, 2008.

[8] E. J. Rodriguez-Seda, "Decentralized trajectory tracking with collision avoidance control for teams of unmanned vehicles with constant speed," in *American Control Conference (ACC), 2014*. IEEE, 2014, pp. 1216–1223.

[9] P. Panyakeow and M. Mesbahi, "Decentralized deconfliction algorithms for unicycle uavs," in *American Control Conference (ACC), 2010*. IEEE, 2010, pp. 794–799.

[10] B. Di, R. Zhou, and H. Duan, "Potential field based receding horizon motion planning for centrality-aware multiple uav cooperative surveillance," *Aerospace Science and Technology*, vol. 46, pp. 386–397, 2015.

[11] M. Defoort, A. Kokosy, T. Floquet, W. Perruquetti, and J. Palos, "Motion planning for cooperative unicycle-type mobile robots with limited sensing ranges: A distributed receding horizon approach," *Robotics and autonomous systems*, vol. 57, no. 11, pp. 1094–1106, 2009.

[12] J. Shin and H. J. Kim, "Nonlinear model predictive formation flight," *IEEE Transactions on Systems, Man, and Cybernetics-Part A: Systems and Humans*, vol. 39, no. 5, pp. 1116–1125, 2009.

[13] C. Tomlin, G. J. Pappas, and S. Sastry, "Conflict resolution for air traffic management: A study in multiagent hybrid systems," *IEEE Transactions on automatic control*, vol. 43, no. 4, pp. 509–521, 1998.

[14] C.-K. Lai, M. Lone, P. Thomas, J. Whidborne, and A. Cooke, "On-board trajectory generation for collision avoidance in unmanned aerial vehicles," in *Aerospace Conference, 2011 IEEE*. IEEE, 2011, pp. 1–14.

[15] Y. Lin and S. Saripalli, "Path planning using 3d dubins curve for unmanned aerial vehicles," in *Unmanned Aircraft Systems (ICUAS), 2014 International Conference on*. IEEE, 2014, pp. 296–304.

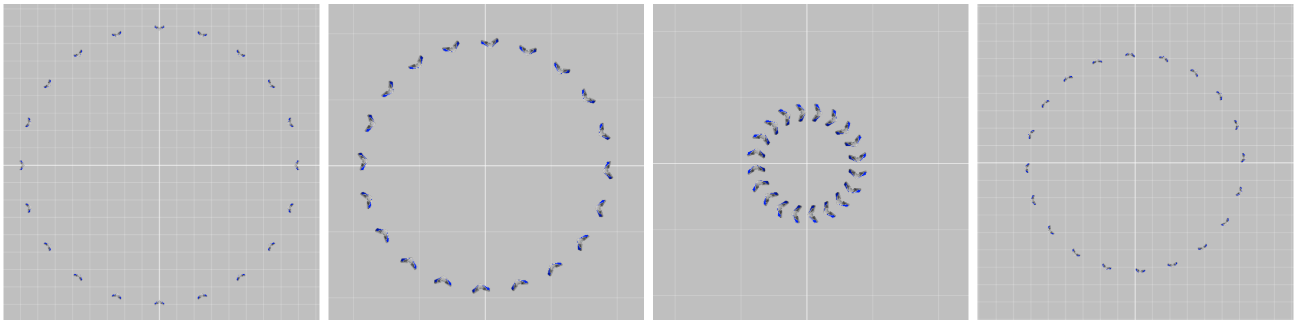

(a) (b) (c) (d)

Fig. 5: A demonstration of 20 fixed-wing vehicles applying barrier certificates to ensure collisions are avoided when constructing h defined in (9) by γ_{turn}. (a) The starting position of 20 vehicles. (b) The vehicles approach the origin and begin avoidance behavior around 50 meters away from the origin. (c) The vehicles circle the origin. (d) The vehicles reach approach their target position.

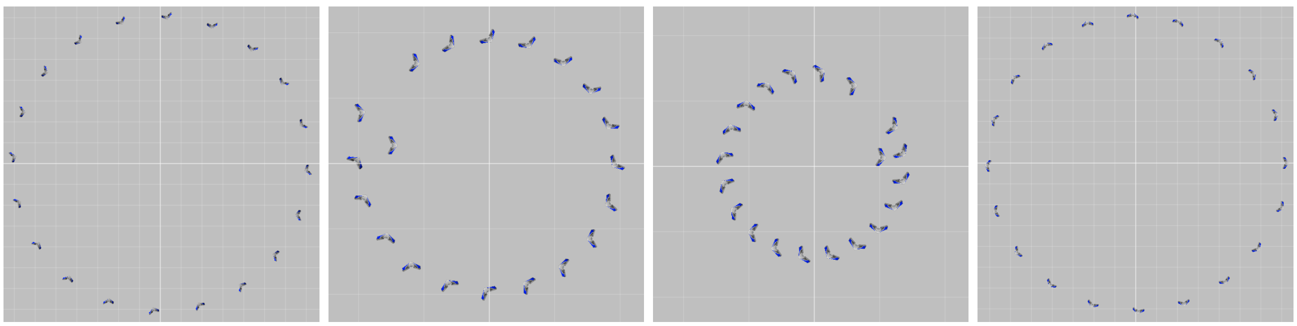

(a) (b) (c) (d)

Fig. 6: A demonstration of 20 fixed-wing vehicles applying barrier certificates to ensure collisions are avoided when constructing h defined in (9) by $\gamma_{straight}$. (a) The starting position of 20 vehicles. (b) The vehicles approach the origin and begin avoidance behavior around 50 meters away from the origin. (c) The vehicles circle the origin. (d) The vehicles reach approach their target position. The asymetry is due to the fact that the vehicles have different speeds for their nominal evading maneuvers. As the speed for the nominal maneuvers approaches the same value the result is a more symmetric pattern.

[16] ——, "Collision avoidance for uavs using reachable sets," in *Unmanned Aircraft Systems (ICUAS), 2015 International Conference on*. IEEE, 2015, pp. 226–235.

[17] L. Pallottino, V. G. Scordio, A. Bicchi, and E. Frazzoli, "Decentralized cooperative policy for conflict resolution in multivehicle systems," *IEEE Transactions on Robotics*, vol. 23, no. 6, pp. 1170–1183, 2007.

[18] A. Krontiris and K. E. Bekris, "Using minimal communication to improve decentralized conflict resolution for non-holonomic vehicles," in *Intelligent Robots and Systems (IROS), 2011 IEEE/RSJ International Conference on*. IEEE, 2011, pp. 3235–3240.

[19] S. Prajna, "Barrier certificates for nonlinear model validation," *Automatica*, vol. 42, no. 1, pp. 117–126, 2006.

[20] A. D. Ames, X. Xu, J. W. Grizzle, and P. Tabuada, "Control barrier function based quadratic programs for safety critical systems," *IEEE Transactions on Automatic Control*, vol. 62, no. 8, pp. 3861–3876, 2017.

[21] U. Borrmann, L. Wang, A. D. Ames, and M. Egerstedt, "Control barrier certificates for safe swarm behavior," *IFAC-PapersOnLine*, vol. 48, no. 27, pp. 68–73, 2015.

[22] L. Wang, A. D. Ames, and M. Egerstedt, "Safe certificate-based maneuvers for teams of quadrotors using differential flatness," *arXiv preprint arXiv:1702.01075*, 2017.

[23] Q. Nguyen and K. Sreenath, "Safety-critical control for dynamical bipedal walking with precise footstep placement," *IFAC-PapersOnLine*, vol. 48, no. 27, pp. 147–154, 2015.

[24] S.-C. Hsu, X. Xu, and A. D. Ames, "Control barrier function based quadratic programs with application to bipedal robotic walking," in *American Control Conference (ACC), 2015*. IEEE, 2015, pp. 4542–4548.

[25] X. Xu, J. W. Grizzle, P. Tabuada, and A. D. Ames, "Correctness guarantees for the composition of lane keeping and adaptive cruise control," *IEEE Transactions on Automation Science and Engineering*, 2017.

[26] X. Xu, P. Tabuada, J. W. Grizzle, and A. D. Ames, "Robustness of control barrier functions for safety critical control," *IFAC-PapersOnLine*, vol. 48, no. 27, pp. 54–61, 2015.

[27] X. Xu, T. Waters, D. Pickem, P. Glotfelter, M. Egerstedt, P. Tabuada, J. W. Grizzle, and A. D. Ames, "Realizing simultaneous lane keeping and adaptive speed regulation on accessible mobile robot testbeds," in *Control Technology and Applications (CCTA), 2017 IEEE Conference on*. IEEE, 2017, pp. 1769–1775.

[28] L. Wang, A. D. Ames, and M. Egerstedt, "Multi-objective compositions for collision-free connectivity maintenance in teams of mobile robots,"

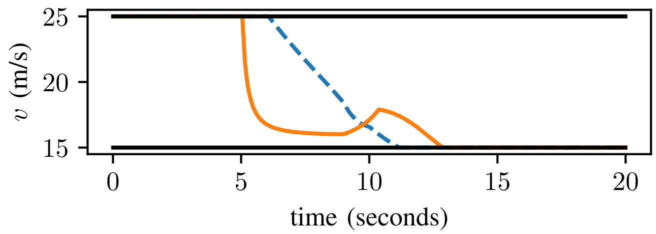

(a)

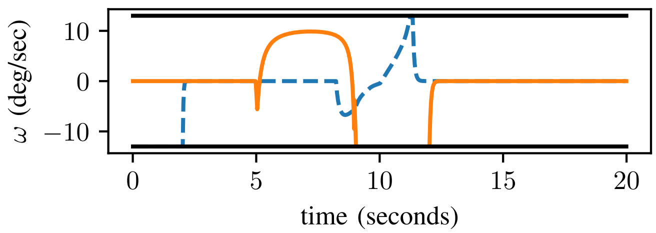

(b)

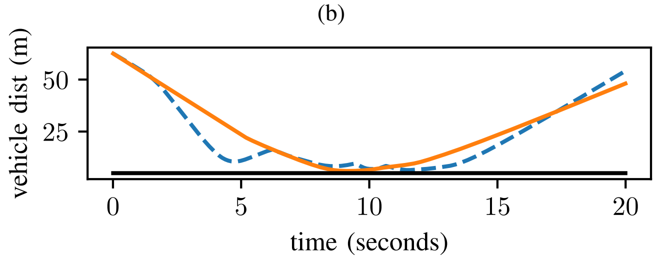

(c)

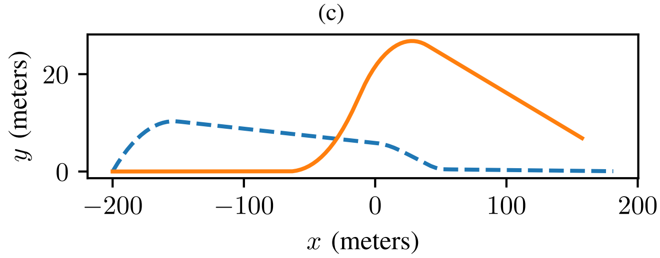

(d)

Fig. 7: Outputs for the scenario with 20 fixed-wing vehicles. The blue dashed and orange solid lines are the output of the scenario where h is constructed from $\gamma_{straight}$ and γ_{turn}, respectively. Vehicle 1 velocity and turn rates are shown to be within the actuator limits in (a) and (b). Vehicle 1 is plotted as a representative output since all 20 vehicles cannot be shown on the same plot. In (c), the minimum distance between any two vehicles is shown to be above D_s. (d) is the path taken by vehicle 1. Note that the behavior is significantly different when constructing h with γ_{turn} and $\gamma_{straight}$.

in *Decision and Control (CDC), 2016 IEEE 55th Conference on*. IEEE, 2016, pp. 2659–2664.

[29] S. Prajna and A. Jadbabaie, "Safety verification of hybrid systems using barrier certificates," in *HSCC*, vol. 2993. Springer, 2004, pp. 477–492.

[30] L. Wang, D. Han, and M. Egerstedt, "Permissive barrier certificates for safe stabilization using sum-of-squares," *arXiv preprint arXiv:1802.08917*, 2018.

[31] P. A. Parrilo, "Semidefinite programming relaxations for semialgebraic problems," *Mathematical programming*, vol. 96, no. 2, pp. 293–320, 2003.

[32] Q. Nguyen and K. Sreenath, "Exponential control barrier functions for enforcing high relative-degree safety-critical constraints," in *American Control Conference (ACC), 2016*. IEEE, 2016, pp. 322–328.

[33] X. Xu, "Constrained control of input–output linearizable systems using control sharing barrier functions," *Automatica*, vol. 87, pp. 195–201, 2018.

[34] P. Glotfelter, J. Cortés, and M. Egerstedt, "Nonsmooth barrier functions with applications to multi-robot systems," *IEEE control systems letters*, vol. 1, no. 2, pp. 310–315, 2017.

[35] E. Squires, P. Pierpaoli, and M. Egerstedt, "Constructive barrier certificates with applications to fixed-wing aircraft collision avoidance," in *Control Technology and Applications (CCTA), 2018 IEEE Conference on*. IEEE, 2018.

[36] K. DeMarco, E. Squires, M. Day, and C. Pippin, "Simulating collaborative robots in a massive multi-agent game environment (SCRIMMAGE)," in *Int. Symp. on Distributed Autonomous Robotic Systems*, 2018.

[37] R. Olfati-Saber, "Near-identity diffeomorphisms and exponential/spl epsi/-tracking and/spl epsi/-stabilization of first-order nonholonomic se (2) vehicles," in *American Control Conference, 2002. Proceedings of the 2002*, vol. 6. IEEE, 2002, pp. 4690–4695.

[38] L. J. Clancy, *Aerodynamics*. Halsted Press, 1975.

[39] B. Stellato, G. Banjac, P. Goulart, A. Bemporad, and S. Boyd, "OSQP: An operator splitting solver for quadratic programs," *ArXiv e-prints*, Nov. 2017.

[40] B. Morris, M. J. Powell, and A. D. Ames, "Sufficient conditions for the lipschitz continuity of qp-based multi-objective control of humanoid robots," in *Decision and Control (CDC), 2013 IEEE 52nd Annual Conference on*. IEEE, 2013, pp. 2920–2926.

[41] T. C. Sideris, *Ordinary differential equations and dynamical systems*. Springer, 2013.